Planta (2007) 225:1107–1120
DOI 10.1007/s00425-006-0420-z

ORIGINAL ARTICLE

Underexpression of the plant *NOTCHLESS* gene, encoding a WD-repeat protein, causes pleitropic phenotype during plant development

Sier-Ching Chantha · Daniel P. Matton

Received: 23 August 2006 / Accepted: 29 September 2006 / Published online: 4 November 2006

Abstract WD-repeat proteins are involved in a breadth of cellular processes. While the WD-repeat protein encoding gene *NOTCHLESS* has been involved in the regulation of the Notch signaling pathway in *Drosophila*, its yeast homolog Rsa4p was shown to participate in 60S ribosomal subunit biogenesis. The plant homolog *ScNLE* was previously characterized in *Solanum chacoense* (*ScNLE*) as being involved in seed development. However, expression data and reduced size of *ScNLE* underexpressing plants suggested in addition a role during shoot development. We here report the detailed phenotypic characterization of *ScNLE* underexpressing plants during shoot development. *ScNLE* was shown to be expressed in actively dividing cells of the shoot apex. Consistent with this, *ScNLE* underexpression caused pleiotropic defects such as a reduction in aerial organ size, a reduction in some organ numbers, delayed flowering, and an increase in stomatal index. Analysis of adaxial epidermal cells revealed that both cell number and cell size were reduced in mature leaves of *ScNLE* underexpressing lines. Two-hybrid screens with the Nle domain and the WD-repeat domain of ScNLE allowed the isolation of homologs of yeast *MIDASIN* and *NSA2* genes, the products of which are involved in 60S ribosomal subunit biogenesis in yeast. A ScNLE-GFP chimeric protein was localized in both the cytoplasm and nucleus. These data altogether suggest that ScNLE likely plays a role in 60S ribosomal subunit biogenesis, which is essential for proper cellular growth and proliferation during plant development.

Keywords Notchless · WD-repeat protein · Meristem · Stomata · Midasin · Ribosome biogenesis

Genbank Accession number ScNle: AY428810

Abbreviations
DAP Days after pollination
HAP Hours after pollination
SAM Shoot apical meristem

Introduction

In animals, adult organs are initiated during embryogenesis while in plants, new organs are continuously generated post-embryonically through meristematic cell sources. The shoot apical meristem (SAM) is pivotal for shoot development as it maintains a population of undifferentiated cells while also contributing the cells required for lateral organ primordia and stem formation throughout plant development (Esau 1977). Cells initially recruted to organ primordia retain their meristematic competence but only for a limited period of time. Subsequent gradual loss of cell meristematic competence during organ maturation is combined with cell growth/expansion and differentiation. The final size of a plant organ therefore reflects both cell number and cell size composition (Mizukami 2001).

Cell growth and cell division require the expression of a large number of genes involved in basic cellular functions. Members of the WD-repeat (WDR) protein

S.-C. Chantha · D. P. Matton (✉)
Département de Sciences Biologiques,
Institut de Recherche en Biologie Végétale (IRBV),
Université de Montréal, 4101 rue Sherbrooke Est,
Montréal, QC, Canada H1X 2B2
e-mail: dp.matton@umontreal.ca

superfamily, found almost exclusively in eukaryotes, have been involved in cellular processes as diverse as cytoskeletal dynamics, vesicular traffiking, nuclear export, RNA processing, chromatin modification, signal transduction, and ribosome biogenesis, to name a few examples (Neer et al. 1994; van Nocker and Ludwig 2003). Although functionally diversified, WDR proteins are structurally related by sharing the WD-repeat as a common sequence motif, which is repeated from four to sixteen times within a protein (Smith et al. 1999). They are thought to fold altogether into a propeller-like structure that would serve as a stable platform to coordinate the specific interaction of multiple protein partners in simultaneous and/or in a successive manner (Smith et al. 1999), a feature that could allow WDR proteins to integrate molecular mechanisms and pathways.

In *Arabidopsis*, 237 WRD proteins were grouped into 143 distinct families, the majority of which are evolutionary conserved in animals, plants and yeast, suggesting that many of them are components of basic cellular mechanisms (van Nocker and Ludwig 2003). Only few of these members have been characterized to date for their function during plant growth and development. One intriguing WDR member is the homolog of the *Drosophila melanogaster NLE* (*DmNLE*) gene. *DmNLE* was first characterized as a modifier of the transmembrane Notch receptor activity in *Drosophila* (Royet et al. 1998). The DmNLE protein was shown to interact directly with the cytoplasmic domain of Notch, but the mechanism by which it regulates the activity of the receptor remains unclear. In animals, numerous cell fate decisions and developmental processes rely on cellular signaling through the Notch pathway (Kimble and Simpson 1997). In plants and yeast however, a Notch-type receptor and other components associated to the signaling pathway appear to be absent (Wigge and Weigel 2001). The yeast *NLE* homolog gene product, also known as Rsa4p and YCR072p, was later found as a *trans*-acting factor associated to pre-60S ribosomal particles throughout their maturation, from the nucleolus to the cytoplasm (Bassler et al. 2001; Gavin et al. 2002; Nissan et al. 2002). Yeast NLE/Rsa4p was shown to be required for proper rRNA processing and intranuclear transport of pre-60S ribosomal particles (de la Cruz et al. 2005). Most of the *trans*-acting factors involved in ribosome biogenesis have been characterized in *Saccharomyces cerevisiea* but the conservation of almost all these factors in higher eukaryotes suggest that ribosome biogenesis process is conserved in plants, animals, and fungi (Tschochner and Hurt 2003). However, reports on the role of genes encoding *trans*-acting factors involved in ribosome maturation during plant development are scarce.

A plant *NLE* homolog was previously isolated in a subtractive screen as a gene that is transiently up-regulated by fertilization in the ovaries of *Solanum chacoense*, a wild potato species, and was characterized for its function in post-fertilization processes (Chantha et al. 2006). *ScNLE* was shown to be expressed in diverse tissues of the ovary after fertilization, including the endothelium of ovules, placenta, and vascular tissues. Underexpressing *ScNLE* in transgenic plants led to the production of smaller fruits containing high proportions of aborted ovules and seeds. However, this also led to the production of smaller plants, suggesting an involvement of *ScNLE* during shoot development as well. We herein report a detailed characterization of the defects associated to shoot development and aerial organ formation in *ScNLE* underexpressing lines. We propose that these developmental defects originate from the requirement of *ScNLE* for proper cell growth and cell proliferation, and an implication in a basic cellular process. Results from our two-hybrid screens also provide further support to the participation of the *NLE* gene in ribosome biogenesis in plants.

Materials and methods

Plant material and growth conditions

The diploid ($2n = 2x = 24$) *S. chacoense* Bitt. (Potato Introduction Station, Sturgeon Bay, WI, USA) self-incompatible genotypes were line G4 (S_{12} and S_{14} self-incompatibility alleles) as female progenitor and line V22 (S_{11} and S_{13} alleles) as pollen donor. Plants were maintained by *in vitro* propagation on 0.5 time MS medium with charcoal (0.5 time MS salts, one time MS vitamins, 20% sucrose, 0.5% deactivated charcoal, 0.6% agar, pH 5.8) at 20–22 °C with a photoperiod of 16 h light and 8 h dark. Plants from 1 to 2 months old were transferred to soil and were grown either in a greenhouse with an average of 14 h of light/day for flower analyses or in a growth chamber at 20–22 °C with a photoperiod of 16 h light and 8 h darkness for comparative examination of vegetative growth parameters.

In situ hybridization and GUS analysis

For in situ hybridization, tissue samples were fixed, dehydrated and embedded in paraffin as described previously (Lantin et al. 1999). In situ detection of *ScNLE* on 10 µm thick sections was performed as described previously (Lantin et al. 1999). Sense and antisense digoxigenin-11-UTP (Roche Diagnostics, Laval, QC, Canada) labeled riboprobes were synthesized from the

ScNLE cDNA cloned in the pBK-CMV vector using T3 and T7 RNA polymerases (RNA transcription kit, Stratagene, LaJolla, CA, USA) after linearisation of the plasmid with *Xho*I or *Eco*RI, respectively. For GUS analysis, details on *ScNLE* promoter cloning and GUS staining are provided in Chantha et al. (2006).

Microscopy

Plant material embedded in paraffin was prepared for sectioning as described for in situ hybridization. For leaf cell morphology analysis, sections were rehydrated and stained with safranine overnight, thoroughly washed in water and then stained with Astra blue for 20 min. After two washes in water, sections were dehydrated. Methods for *ScNLE* promoter-GUS fusion construct and GUS staining are detailed in Chantha et al. (2006). Tissue sections 10 µm thick were mounted in Permount. Adaxial epidermal cells were analyzed from nail polish peels. Nail polish was applied on the central region of terminal leaves surface and, once dried, peeled by using adhesive tape. Peels were sticked on microscope slides. Images were acquired with a digital camera installed on a Leitz light microscope.

ScNLE constructs for underexpression

For gene suppression using the antisense strategy, a ~1500 bp fragment of *ScNLE* cDNA was cloned in the antisense orientation in the pBIN35S double-enhancer vector using the *Hin*dIII restriction sites (Bussiere et al. 2003). For gene suppression using the double-stranded RNA interference strategy, a ~650 bp fragment of *ScNLE* cDNA was cloned in the sense and antisense orientations in the pDarth vector (O'Brien et al. 2002) from PCR products obtained with the NLE14 (5′-GAGAGGATCCAAACCACGCAGGGGAAGCTA-3′) and NLE18 (5′-GAGAGGCGCGGTACCCTATCCCATCCATAGCTTCAG) primers containing the *Bam*HI and *Xho*I restriction sites, respectively, and with the NLE19 (5′-GAGACTCGAGAAACCACGCAGGGGAAGCTA-3′) and NLE22 (5′-GAGAGGCGCGCCCTATCCCATCCATAGCTTCAG-3′) primers containing the *Xho*I and *Asc*I restriction sites, respectively. Plant transformation with *Agrobacterium tumefaciens* strain LBA4404 was carried out as described previously (Matton et al. 1997).

Two-hybrid cDNA libraries synthesis

Isolation of total RNA and poly(A)$^+$ mRNA were performed as described previously (Lantin et al. 1999). An AD-cDNA target library was synthetized from 5 µg of poly(A)$^+$ mRNA isolated from ovaries collected 18–72 HAP in the pAD-GAL4-2.1 phagemid vector by using the HybriZap®-2.1 XR library construction kit (Stratagene), according to the manufacturer's instructions. The activation domain-tagged primary cDNA library contained 1.6×10^6 independent clones. A MYR-cDNA target library was synthetized from 5 µg of poly(A)$^+$ mRNA isolated from depericarped ovaries collected two to six DAP in the pMyr XR vector using the CytoTrap® XR Library construction kit (Stratagene), according to the manufacturer's instructions.

ScNLE constructs for two-hybrid screens

For all the two-hybrid constructs, sequences were amplified from *ScNLE* cDNA using PWO DNA Polymerase (Roche Diagnostics). All constructs were sequenced to confirm that fusions were in-frame and unmutated.

The vector pBD GAL4 Cam (Stratagene) was used to construct C-terminal fusions of three ScNLE regions with the binding domain of GAL4 and generate the following bait proteins: BD-dNLE (Nle domain), BD-dWD (WDR domain) and BD-ScNLE (complete ScNLE protein). Primers used for PCR amplification were tagged with *Eco*RI and *Sal*I restriction site sequences in the forward and reverse primers, respectively. The Nle domain (aa 2–115) was amplified with the NLE4 (5′-CG**GAATTC**GAAGTGGAAGTGGAAGCT-3′) and NLE6 (5′-CGTA**GTCGAC**CAGCAATTGTGGCCGAA-3′) primers. The WDR domain (aa 101–482) was amplified with the NLE23 (5′-GAGA**GAATTC** TTTCGAATCCGCCCTGTCAC-3′) and NLE8 (5′-CAT**GTCGAC**CTATCCCATCCATAGCTTCAG-3′) primers. The full ScNLE coding region, excluding the initiation codon, was amplified with the NLE4 and NLE8 primers. PCR products were digested with and ligated to the *Eco*RI and *Sal*I sites of pBD GAL4 Cam.

The vector pSos (Stratagene) was used to construct C-terminal fusions of the three same ScNLE regions (mentioned above) with Sos to generate the following bait proteins: Sos-dNLE, Sos-dWD and Sos-ScNLE. The primers used for PCR amplification were tagged with the *Bam*HI and *Sal*I restriction site sequences in the forward and reverse primers, respectively. The Nle domain was amplified with the NLE11 (5′-CG**GGATCC**GAAGTGGAAGTGGAAGCT-3′) and NLE6 primers. The WDR domain (nt 402 to stop codon; aa 110–482) was amplified with the NLE12 (5′-GAGA**GGATCC**GTTCGGCCACAATTGCTGGT-3′) and NLE8 primers. The full ScNLE ORF was amplified with the NLE11 and NLE8 primers. PCR products

were digested with and ligated to the *Bam*HI and *Sal*I sites of pSos.

Two-hybrid screening

GAL4 system

Bait plasmids were separately transformed into yeast strain PJ69-4A (kindly provided by Phillip James, University of Wisconsin Medical School, Madison, WI, USA) (James et al. 1996). Yeast strains carrying BD fusion plasmids were transformed with the pAD-GAL4-2.1 library according to a modified version of the high efficiency lithium acetate method of Agatep et al. (1998). Transformed cells were plated on synthetic complete (SC) medium—Leu-Trp-His supplemented with 1 mM 3-amino-1′,2′,4′-triazole (3AT) and incubated at 30 °C for 14 days. Colonies were replica-plated on SC medium—Leu-Trp-Ade and incubated at 30 °C for an additional 14 days. Autoactivating target plasmids were eliminated by segregation analysis and plasmid DNA was extracted from positive colonies (Parchaliuk et al. 1999). Yeast plasmid DNA was transformed into electrocompetent XL1-blue MRF' (Stratagene) and cells with pAD target plasmid were selected on LB agar plates containing 100 μg/ml ampicillin. Positive target plasmids were separately transformed back into PJ69-4A harboring the pBD-GAL4 Cam, pBD-dNLE, pBD-dWD, or pBD-ScNLE plasmid for reconstruction of two-hybrid positives. A rapid LiAc transformation protocol was used for yeast transformation with bait and positive target plasmids (Gietz and Woods 2002).

Sos recruitment system

Bait plasmids were cotransformed with pMyr target library in the temperature-sensitive yeast strain cdc25H according to the CytoTrap instruction manual (Stratagene). Transformed cells were plated on SC/glucose medium—Ura-Leu and incubated at 25 °C for 2 days. Colonies were replica-plated on SC medium/galactose—Ura-Leu and incubated at 37 °C for 10 days. Positive colonies were selected and positive interaction clones were confirmed as specified in the CytoTrap instruction manual. The cDNA inserts isolated from positive colonies were sequenced.

Isolation and gel blot analysis of RNA

Isolation of total RNA as well as gel blot analyses were performed as described previously (Lagacé et al. 2003; Lantin et al. 1999). A 10 μg of total RNA for each tissue samples were separated on gel. Probes were derived from partial *ScMDN1* cDNA labelled with α-[^{32}P]-dATP (ICN Biochemicals, Irvine, CA, USA) using the High Prime DNA Labeling kit (Roche Diagnostics, Laval, QC, Canada). A ^{32}P-labelled *18S* probe was used as a control. Membranes were exposed at -85 °C with intensifying screens on Kodak Biomax MR film (Interscience, Markham, ON, Canada).

Protoplast transformation and GFP visualization

ScNLE-eGFP was expressed as a translational fusion under the control of the CaMV 35S promoter. Protoplasts were derived from *Nicotiana tabacum* leaf mesophyll cells as described previously (Koop et al. 1996). Protoplasts were transformed with 40 μg of plasmid with a Cell PORATOR apparatus (Gibco BRL, Burlington, ON, Canada) with voltage adjusted to 225 V and the capacitor to 1000 μF. Live protoplasts were observed on microscope slides 24 h after incubation in culture medium. Images were acquired using a Leica TCS SP1 laser scanning confocal microscope. An argon laser emitting at 488 nm was used as the light source. GFP fluorescence and chlorophyll autofluorescence were detected in separate channels at 500–530 and 670–700 nm, respectively. The laser intensity was limited in order to minimize photobleaching. Under these conditions, no GFP fluorescence was detected in control untransformed protoplasts. For display, GFP and chlorophyll images were pseudo-colored in green and red, respectively, and overlaid using the Leica Confocal Software (LCS). The corresponding Nomarski images were acquired simultaneously.

DNA sequencing and analysis

Approximately 200 ng (5 μl) of plasmid DNA and 15 μl of reaction mixture containing 8.5 μl of water, 3.5 μl five times sequencing buffer, 2 μl primer at 0.8 μM, and 1 μl Big Dye Terminator Ready Reaction Mix (PE Applied Biosystems) was used for the sequencing reaction. Sequencing reactions were preformed on a GeneAmp PCR System 9700 (PE Applied Biosystems), and the cycling conditions were: 96 °C, 10 s; 50 °C, 5 s; 60 °C, 4 min for 25 cycles. DNA sequencing was performed on an Applied Biosystem ABI 310 or 3100 automated sequencer. Sequence alignments were performed with the ClustalW module of the MacVector 7.2.3 software (Accelrys). Database searches were conducted with the BLAST program at The *Arabidopsis* Information Resource (www.arabidopsis.org) and at the National Center for Biotechnology Information (www.ncbi.nlm.nih.gov). Cellular localizations were

predicted using PSORT (www.psort.nibb.ac.jp) and SignalP (www.cbs.dtu.dk/services/SignalP).

Results

ScNLE is expressed in actively dividing cells of the shoot apex

ScNLE has previously been shown by RNA gel blot analysis to be expressed in the shoot apex (Chantha et al. 2006). In situ hybridization was performed to define more precisely its expression pattern. In shoot apex sections, *ScNLE* localization was associated to actively dividing cells (Fig. 1). *ScNLE* transcripts were detected in the shoot apical and axillary meristems (Fig. 1a), in inflorescence meristems (Fig. 1b), in growing zones of young developing leaves, in floral organ primordia, as well as in the procambium (Fig. 1a, b). Analysis of plants transformed with a translational fusion of an about 1,100 bp *ScNLE* promoter fragment to GUS revealed identical staining patterns in the shoot apex in addition to expression in the veins of young leaves (Fig. 1d). Such expression pattern suggests that *ScNLE* plays a role in actively dividing cells during shoot development and aerial organ formation.

Reducing *ScNLE* expression levels in *S. chacoense* causes a pleiotropic phenotype

To investigate the function of *ScNLE* during shoot development, we analyzed the phenotypes of four transgenic lines underexpressing *ScNLE* that were generated previously with antisense or double-stranded RNA constructs (Chantha et al. 2006). These lines, namely asNLE3, asNLE5, iNLE5, and iNLE6, shared similar pleiotropic phenotypes although with different degrees of severity, with asNLE5 and iNLE6 showing overall the strongest developmental defects.

ScNLE underexpression led to a considerable array of developmental alterations. The most striking effect was an overall reduction in plant size (see Fig. 7a in Chantha et al. 2006) that was reflected by a reduction in the size of all the aerial organs examined. Height of

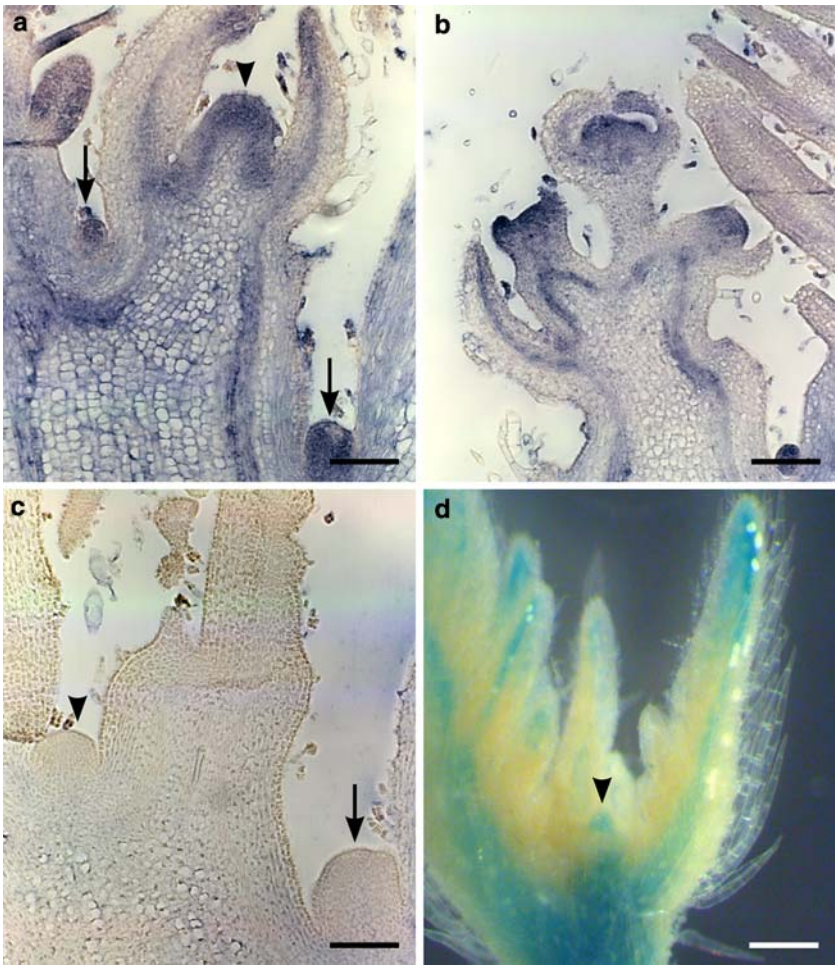

Fig. 1 In situ localization of *ScNLE* transcripts in the apex. **a** Vegetative apex, longitudinal section, *ScNLE* antisense probe. **b** Inflorescence apex, longitudinal section, *ScNLE* antisense probe. **c** Vegetative apex, longitudinal section, *ScNLE* sense probe. **a**–**c** Bar = 100 μm. **d** GUS staining pattern conferred by *ScNLE* promoter Bar = 250 μm. In **a**, **c** and **d**, *arrowheads* indicate shoot apical meristems and arrows indicate axillary meristems.

ScNLE underexpressing plants, represented by stem length, was constantly lower than the WT (Fig. 2a) and stem width was correspondingly smaller (Fig. 2d). Moreover, *ScNLE* underexpressing plants produced smaller leaves, with both reduced blade width and length (Fig. 2c). Measurement of total leaf surface area produced by 9-week-old plants revealed that this reduction represented ~12% in iNLE5 to ~85% in asNLE3 (248 ± 11.5 to 41.9 ± 19.4 cm^2, $n = 10$ and 6, respectively) of the WT value (281 ± 21.3 cm^2, $n = 10$). Young asNLE3 plants were chlorotic and had an etiolated phenotype that could explain the discrepancy between severe reduction in leaf size (Fig. 2c) and mild phenotype on plant height (Fig. 2a). However asNLE3 plants recovered from this chlorosis defect in later development stages but still maintained the reduced size and other phenotypes discussed below. The significant reduction in total leaf surface area (*t*-test, $p < 0.001$) was not caused by lower numbers of leaves produced per plant since the rates of leaf production were similar or even higher in *ScNLE* underexpressing plants compared to the WT throughout plant development (Fig. 2b). Reduction in size was also observed for flower organs (Fig. 2e). These observations altogether show that *ScNLE* underexpression caused an overall reduction in aerial organ size.

Reducing *ScNLE* expression also reduced the number of some organs formed. For example, *ScNLE* underexpressing plants produced compound leaves with fewer leaflets than WT leaves at equivalent positions (Fig. 2c). Moreover, their stems did not produce the ridges normally formed along the mature WT stem that are apparently associated to larger vascular bundles in *S. chacoense* (Fig. 2d). In *ScNLE* underexpressing lines, the size of the vascular bundles seemed to be insufficient to trigger the formation of such ridges. Flowers of *ScNLE* underexpressing lines also showed a variety of organ defects. In the case of the strong iNLE6 line, flower buds were formed but always dropped at very early stages of their formation. The asNLE5 line, and at a lesser extend the iNLE5 line, produced flowers with four sepals and petals in high proportions while most WT flowers produce five sepals and five petals (Fig. 2e). Petal fusion was also affected, being completely unfused in asNLE5 and iNLE5 flowers while WT petals were partially fused at their base (Fig. 2e). *ScNLE* underexpressing lines also showed reduced fertility. Pollen grains that are normally easy to collect from WT mature dehisced anthers by simple mechanical stimulation, could not be obtained from asNLE5 and iNLE5 anthers. Transition to flowering was also considerably delayed from several days or weeks depending on the *ScNLE* underexpressing line.

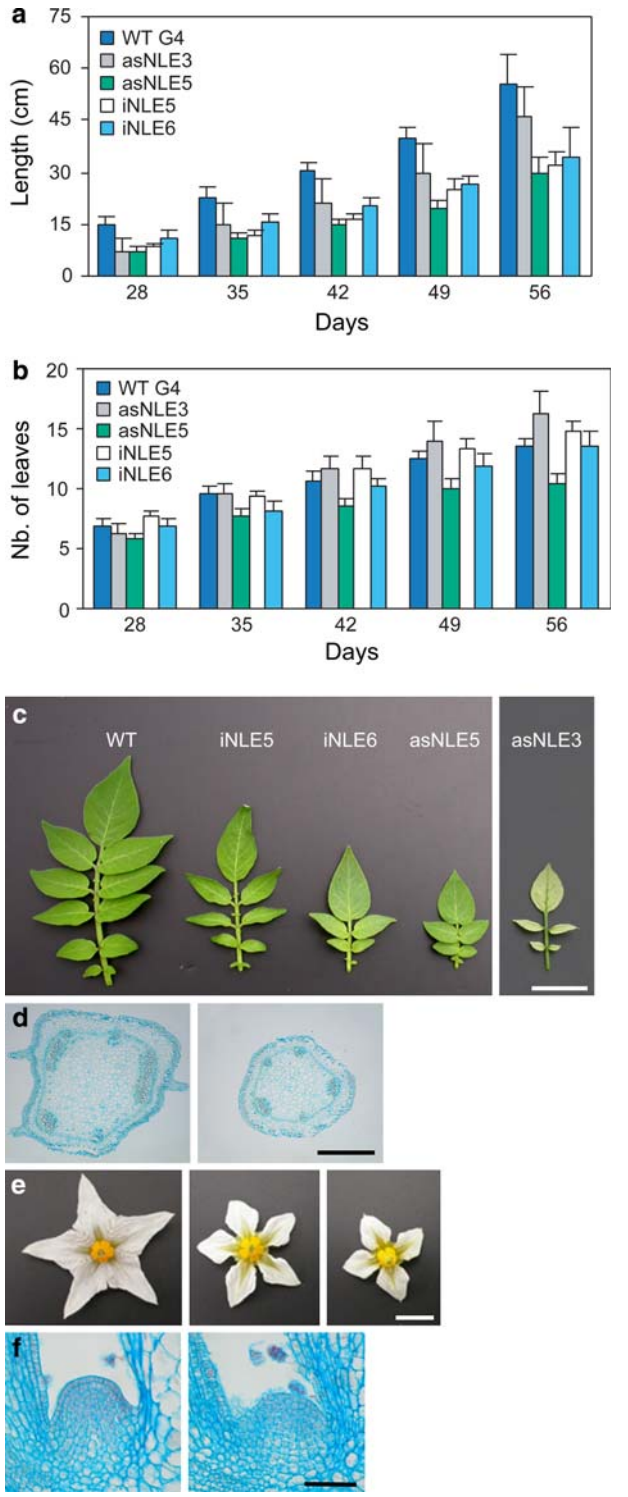

Fig. 2 **a** Stem elongation. Stem lengths of WT and *ScNLE* underexpressing lines were measured 28, 35, 42, 49 and 56 days after transfer of plants from in vitro culture to soil ($n = 10$). **b** Leaf production. Number of opened leaves produced per plant ($n = 10$). **c** Second youngest fully opened leaves of indicated genotype plant. Bar = 2 cm. **d** Transversal sections of WT (*left*) and iNLE6 (*right*) stems. Bar = 1 mm. **e** Morphology of representative flowers of WT (*left*) and iNLE5 line. Bar = 1 cm. **f** Longitudinal sections of WT (*left*) and iNLE6 (*right*) apices. Bar = 50 μm

This pleiotropic shoot phenotype in addition to the expression of *ScNLE* in the shoot apical meristem (SAM) suggested that possible defects in the SAM could have resulted from *ScNLE* underexpression. We therefore analyzed the morphology of the SAM through longitudinal sections of the shoot apex. SAMs of *ScNLE* underexpressing lines showed a typical layered organization although their cell layers were less uniform than in the WT (Fig. 2f). Moreover, SAMs from underexpressing lines were somewhat less protuberant than the WT dome-shaped SAM and therefore seemed smaller (Fig. 2f). This reduction in SAM size may be attributable to a reduced number of meristematic cells since cell size was unaffected (data not shown). All *ScNLE* underexpressing plants continuously produced lateral organs during shoot development, suggesting that meristem maintenance is however not impaired.

ScNLE underexpression leads to alterations in cell size and in cell number

A change in organ size can reflect an alteration in cell size, in cell number, or both. To assess the contributions of cell size and cell number in the production of smaller leaves in *ScNLE* underexpressing lines, adaxial pavement cells of mature leaf blade were analyzed. Comparison with the WT revealed that asNLE3, asNLE5, and iNLE6 lines produced smaller cells (Fig. 3a, b). Surprisingly, the iNLE5 milder underexpressing line produced slightly larger cells (Fig. 3a, b). Cell area measurement showed a significant decrease (*t*-test, $p < 0.001$) from ~70 to ~45% in the asNLE3 and iNLE6 lines (1380 ± 544.6 and 2455 ± 504.1 μm^2, $n = 120$ and 150, respectively) compared to the WT (4316 ± 863.4 μm^2, $n = 150$) (Fig. 3b). Average cell size in iNLE5 line was slightly but significantly larger (4939 ± 940 μm^2, $n = 150$, *t*-test, $p < 0.001$) than the WT (Fig. 3b). Similar results were also obtained with pith cells measured in transversal sections of stems (data not shown). Measurement of adaxial pavement cell area of very young leaves indicated that cells originally produced by *ScNLE* underexpressing lines and the WT were not significantly different in size (Fig. 3b). Since cells originally contributed by the SAM are of similar size, as mentionned above, defects in cell size in *ScNLE* underexpressing leaves occured later during their maturation.

Some observations stemming from our analyses suggested that the reduction in leaf size in *ScNLE* underexpressing lines were not solely caused by a reduction in cell size. iNLE5 epidermal cells were slightly bigger (Fig. 3b) but their leaves were significantly smaller than the WT (Fig. 2c). Moreover, reductions in epidermal cell size in the other *ScNLE* underexpressing lines were not as severe as the reduction in their leaf size. We therefore suspected that cell number could also be affected in transgenic lines underexpressing *ScNLE*. Calculations with the terminal leaflet surface area and the average cell area of mature leaves showed that the average number of adaxial pavement cells was significantly reduced (*t*-test, $p < 0.0001$) by about 35% in all *ScNLE* underexpressing lines compared to the WT (Fig. 3c). Therefore, reduction in cell number contributed to reduced organ size in all *ScNLE* underexpressing lines whereas reduction in cell size contributed only in lines expressing a more severe phenotype. Since surface areas of young leaves in *ScNLE* underexpressing lines were smaller than in the WT (Fig. 2c) while cell sizes were similar at that stage (Fig. 3b), reduced cell number is suggested to originate early during leaf formation, before defects in cell size could be detected.

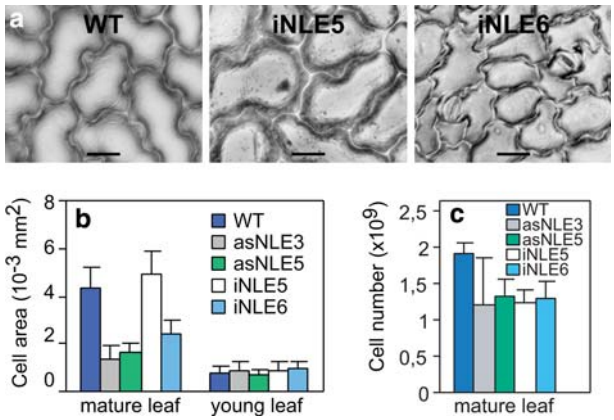

Fig. 3 Adaxial epidermal pavement cell size and cell number in *ScNLE* underexpressing lines. **a** Cell imprints of mature leaf from WT (*left*), iNLE5 (*middle*) and iNLE6 (*right*) lines. Bar = 10 μm. **b** Average cell area of mature and young leaflets of WT and *ScNLE* underexpressing lines. For each line, a total of 150 epidermal cells were measured from ten equivalent terminal leaflets coming from ten independent plants. **c** Total number of cells of mature terminal leaflet. For each line, ten equivalent terminal leaflet areas were measured and divided by corresponding mean cell areas determined in **b**

ScNLE underexpression increases stomatal index

While analyzing the adaxial surface of mature leaves for cell size and cell number determination, we were struck by the high density of stomata found in *ScNLE* underexpressing lines (Fig. 4a, b). Stomatal density, which represents the number of stomata per surface unit, on the adaxial epidermis of mature leaves from all the *ScNLE* underexpressing lines was significantly higher than the WT, with lines asNLE3, asNLE5, and iNLE6 showing more than a fourfold increase (Table 1). Because stomatal density does not take into

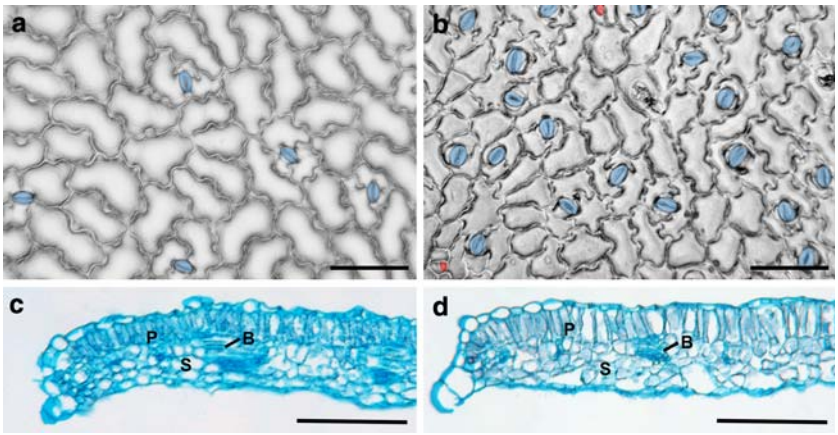

Fig. 4 Stomata production and leaf internal tissues of a *ScNLE* underexpressing line. Adaxial epidermal cell imprints of WT (**a**) and iNLE6 (**b**) mature leaf. Stomata are colored in *blue* and meristemoids are colored in *red*. Transversal sections of mature leaf blades of WT (**c**) and iNLE6 line (**d**). Bars = 100 µm. *P* palisade parenchyma; *S* spongy parenchyma; *B* bundle sheath

Table 1 Stomatal density and stomatal index in WT and various mutant lines

Line	Adaxial leaf			Stem	
	Stomatal density[a]	Stomatal index (%)[b]	Ratio *P*/*S**	Stomatal density[a]	Stomatal index (%)[b]
WT	7.0 ± 2.6	5.8 ± 1.8	17.8 ± 5.2	2.9 ± 1.1	1.6 ± 0.4
asNLE3[c]	34.0 ± 7.7	9.4 ± 2.5	10.3 ± 3.1	6.1 ± 2.1	3.3 ± 1.1
asNLE5	30.2 ± 5.9	9.0 ± 1.6	10.8 ± 2.0	2.8 ± 0.7	2.1 ± 0.6
iNLE5[c]	7.9 ± 1.5[e]	7.7 ± 1.0[d]	12.3 ± 2.0	9.1 ± 3.8	3.2 ± 0.8
iNLE6[c]	40. 9 ± 7.1	15.9 ± 1.1	5.3 ± 0.4	5.2 ± 1.5[d]	2.4 ± 0.3

*P = number of pavement cells; S = number of stomata, ±SD (n = 8 to 13)

[a] Mean total number of stomata per surface unit (0,407 mm^2 field) ± SD (n = 8 to 13)

[b] [si = S / (P + S) * 100] ± SD (n = 8 to 13)

[c] All the values were significantly different from the corresponding WT value (t-test, $p < 0.001$) except for [d, e]

[d] Significantly different from the WT (Student's t-test, $p < 0.01$)

[e] Not significantly different from the WT

account the differences in the size of pavement cells, stomatal index [si = nb of stomata/(nb of pavement cells + nb of stomata) × 100] was also determined. Stomatal index was significantly higher in all *ScNLE* underexpressing lines, being almost up to three-fold higher in iNLE6 adaxial epidermis compared to the WT (Table 1). Therefore, the ratio of pavement cells per stomata (ratio P/S) was decreased in *ScNLE* underexpressing lines (Table 1). To see whether this increase in stomatal index also applied to other organs, we analyzed stomata production on the stem. Stomatal index was also significantly higher on the stem of *ScNLE* underexpressing plants but at a lesser extent than on the leaf (Table 1). These results confirmed that underexpressing *ScNLE* increased the ratio of stomata produced.

To examine whether the structure of internal leaf tissues was affected, sections of mature leaves were analyzed by light microscopy. Leaves typically contain a single layer of elongated parenchyma cells underlying the adaxial epidermis and several layers of spongy parenchyma, composed of cells and air spaces (Fig. 4c). All these cell layers were present in *ScNLE* underexpressing leaves, although spongy parenchyma cells in asNLE3, asNLE5, and iNLE6 (Fig. 4d) were less densely packed compared to the WT, possibly as a consequence of the production of considerably more stomata.

Yeast two-hybrid screens identify MDN1 as a binding partner of ScNLE

In order to determine in which cellular process the ScNLE protein could be involved during plant development, yeast two-hybrid screens were performed to identify ScNLE interacting partners. The Nle domain (dNLE) and the WDR domain (dWD) of ScNLE, both predicted to be involved in protein–protein interactions, were separately used as baits (Fig. 5a). Both the nuclear GAL4 system and the cytoplasmic Sos recruitment (SR) system were used as complementary two-hybrid screening approaches. In the GAL4 system, an AD-cDNA target library of ovaries collected 18–72 HAP was screened with the BD-dNLE and BD-dWD

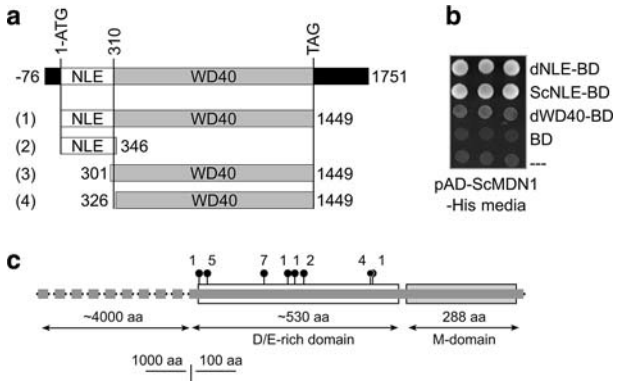

Fig. 5 ScNLE two-hybrid interactions. **a** Schematic representation of *ScNLE* cDNA (*up*). *Numbers* on top represent nucleotide positions, *number 1* corresponding to the first nucleotide of the ATG initiation codon. *Numbers 1–4* represent regions fused to Gal4 BD and/or Sos. *Numbers* on the left and right refer, respectively, to 5′ and 3′ ends of cloned cDNA regions. *1* full ScNLE; *2* Nle domain; *3* WDR domain cloned in pBD-Gal4; *4* WDR domain cloned in pSos. **b** Interactions of pAD-ScMDN1 C-terminal region with different portions of ScNLE fused to Gal4 BD or with Gal4 BD alone in yeast, on—His selection medium. **c** Schematic representation of ScMDN1 with emphasis on its C-terminal region. Circles with associated numbers represent N-terminal position and number of corresponding cDNA clones retrieved from two-hybrid screens with the Nle domain or complete ScNLE protein fused to Gal4-BD or Sos

bait constructs in the yeast strain PJ69-4A. In the SR system, a MYR-cDNA target library of ovaries collected two to six DAP was screened with the Sos-dNLE and Sos-dWD bait constructs in the yeast strain cdc25H. Several candidates were identified of which a homolog of the yeast *MIDASIN* gene (*MDN1*, also known as YLR106c and REA1) was predominantly retrieved with the Nle domain in both two-hybrid systems. Six out of 11 (6/11) and 13 out of 15 (13/15) positive clones representing *ScMDN1* were isolated from screens carried with BD-dNLE (Fig. 5b) and Sos-dNLE, respectively. Interestingly, when the AD-cDNA library was further screened with full-length ScNLE fused to BD, three out of the five positive clones also represented *ScMDN1* (Fig. 5b). However, the WDR domain of ScNLE alone did not interact with ScMDN1 when cotransformed in yeast (Fig. 5b). These results suggest that ScNLE interacted with ScMDN1 through its Nle domain.

MDN1 represents the largest ORF found in the yeast genome, with a predicted sequence of 4,910 aa and molecular mass of 560 kDa (Garbarino and Gibbons 2002) and was shown to be a *trans*-acting factor involved in 60S ribosomal subunit maturation (Galani et al. 2004; Nissan et al. 2004). All the *ScMDN1* clones isolated were therefore only partial cDNAs representing the C-terminal portion of the protein (Fig. 5c). The length of the clones varied from 1,427 to 2,784 bp. The longest cDNA sequence coded for a 816 aa ORF that spanned almost completely the D/E-rich domain and the whole MIDAS domain (M-domain) of MDN1 (Fig. 5c). The shortest cDNA encoded a 364 aa ORF that included only a small C-terminal portion of the D/E-rich domain and the whole M-domain (Fig. 5c). Because all the clones comprised the MIDAS domain but not always the D/E-rich domain, the MIDAS domain is likely to be the one involved in ScMDN1 interaction with ScNLE.

In addition, a homolog of the yeast NSA2 (also known as YER126p) was identified in three out of six (3/6) positive clones in a screen carried with the WDR domain fused to Sos (Sos-dWR) using the SR system. Interestingly, NSA2 was also isolated as a *trans*-acting factor associated to pre-60S ribosomal particles in yeast (Nissan et al. 2002).

ScMDN1 expression pattern in *S. chacoense*

We next performed RNA gel blot analyses to determine *ScMDN1* expression pattern within the plant. We first examined *ScMDN1* expression in various plant organs. Signal was detected in stems, leaves, and shoot apices (including the shoot apical meristem and organ primordia) but not in tubers, roots, petals, anthers and pollen grains (Fig. 6a). Because the expression of ScNLE was previously shown to be induced by fertilization in ovules and ovaries (Chantha et al. 2006), we also analyzed *ScMDN1* expression pattern in these organs in time-course studies following pollination. Figure 6b shows a broad time-course analysis using isolated ovules. Signal was detected in ovules from unpollinated flowers and two days after pollination (DAP) but was very weak or undetectable by four DAP onwards. A more detailed time-course analysis was carried out with pollinated ovaries (Fig. 6c). *ScMDN1* expression was weaker from 12 to 30 h after pollination (HAP), increased at 42 and 48 HAP, and then decreased to basal levels at 72 HAP. In some *Solanaceous* species, including *S. chacoense* (Clarke 1940; Williams 1955; and our unpublished results), the period comprised between 36 and 42 HAP corresponds to the intense basipetal fertilization of the multiple ovules present in the ovary and to initiation of seed development.

A NLE-GFP fusion protein is localized in the cytoplasm and nucleus

Analysis of the ScNLE protein sequence using various prediction tools did not identify any intracellular targeting sequences (e.g. NLS, transit sequence and signal

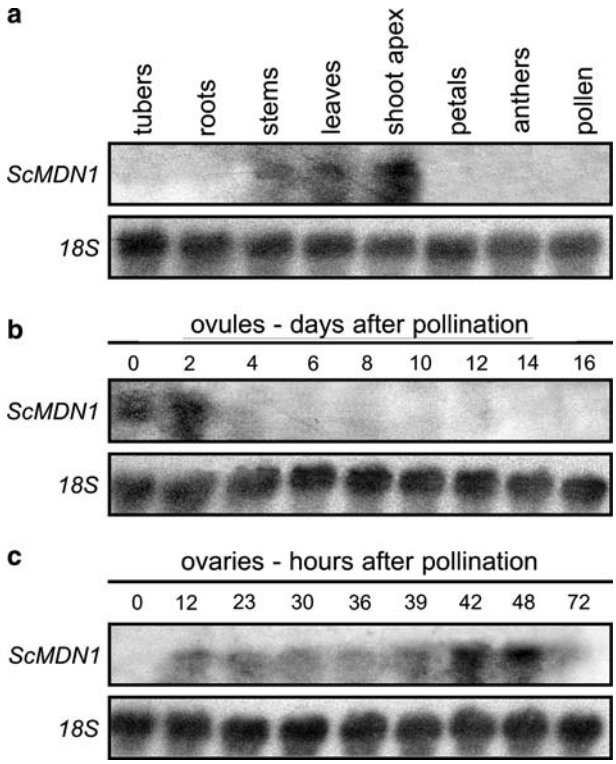

Fig. 6 RNA expression analysis of *ScMDN1* transcript levels. Ten micro gram of total RNA from various tissues were probed with a ^{32}P-labelled *ScMDN1* partial cDNA. **a** Various plant tissues. **b** Dissected ovules at different time points in days after pollination (*DAP*). **c** Ovaries at different time points in hours after pollination (*HAP*). Membranes were stripped and reprobed with a partial 18S ribosomal RNA to assure equal loading of each RNA sample (*lower panel*)

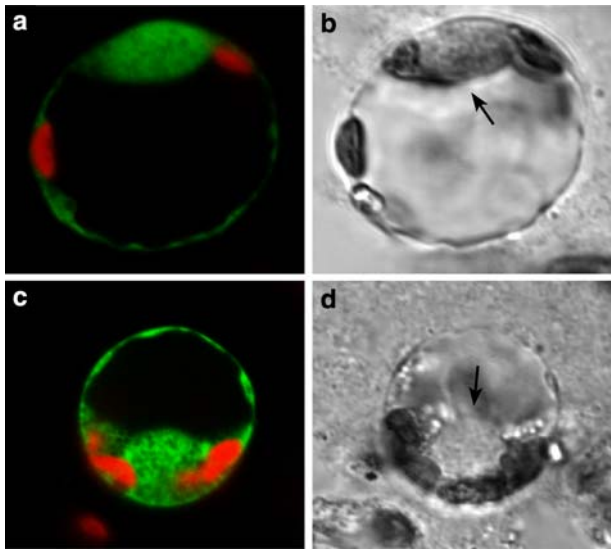

Fig. 7 Transient expression of ScNLE-GFP in tobacco protoplasts. Confocal microscope images of **a** GFP control expression and **c** ScNLE-GFP chimeric protein expression. *Green* represents GFP fluorescence. *Red* represents chlorophyll fluorescence. **b**, **d** Differential interference contrast microscope images of **a** and **c**, respectively. *Arrows* indicate the nucleus

sequence) and therefore predicted a cytoplasmic localization. In order to find out experimentally the cellular localization of ScNLE protein, we expressed a ScNLE-GFP fusion protein driven by the constitutive CaMV 35S promoter in tobacco protoplasts. Surprisingly, the ScNLE-GFP fusion product was not restricted to the cytoplasm but was also found in the nucleus (Fig. 7). Cytoplasmic localization can be seen as a thin ring appressed to the plasma membrane due to the presence of a large vacuole. We therefore considered that ScNLE is distributed in both the cytoplasm and the nucleus.

Discussion

The *ScNLE* gene was originally isolated in a subtractive screen as a gene that is transiently up-regulated in the ovary by fertilization and was previously characterized for its function during post-fertilization events in *S. chacoense* (Chantha et al. 2006). Localization of the gene in the shoot apex as well as reduction in plant size associated with *ScNLE* underexpression however suggested that *ScNLE* is also involved in shoot development, which was the focus of the present study. Also, we provide some evidence that the *ScNLE* gene product, as its yeast homolog, is involved in 60S ribosomal subunit maturation in plants.

Detailed expression studies and phenotypic analysis of underexpressing plants revealed here that *ScNLE* functions in a process that affects cell proliferation and cell enlargement during shoot development. *ScNLE* was shown to be expressed in actively dividing structures of the shoot apex, such as the shoot and floral meristems, organ primordia, and the procambium (Fig. 1). Moreover, underexpressing *ScNLE* led to pleiotropic defects during shoot development, the most prominent ones being an overall reduction in plant aerial organ size and a reduction in some organ numbers (Fig. 2). The final size of a plant organ is determined by cell number (cell proliferation) and cell size (cell enlargement) composition (Mizukami 2001). Analysis of adaxial leaf epidermal pavement cells revealed that aerial organ defects in *ScNLE* underexpressing plants are the consequence primarily of reduced cell number and also of reduced cell size. Reduction in cell number originated very early during leaf formation, possibly at the stage of cell recruitement from the shoot apical meristem (SAM) to primordium anlagen, since *ScNLE* underexpressing plants produced smaller SAMs that contained normal-sized cells (Fig. 2f and data not shown). Also, reduction in cell number was detected

very early during development of *ScNLE* underexpressing leaves, at a stage when sizes of adaxial pavement cells were still indistinguishable from the WT (Fig. 3b). While a reduction in cell number was common to all *ScNLE* underexpressing lines, changes in cell size were not as simply correlated: the less defective iNLE5 line produced larger than normal cells whereas all the other underexpressing lines produced smaller than normal cells. In plants, final organ size would be determined at the whole organ level through a total organ-size checkpoint that coordinates cell proliferation with cell enlargement to ensure that organs reach a determined size (Tsukaya 2002). There are several examples of plant cell cycle progression mutants in which a reduction in cell number in an organ is compensated by an increase in cell size, similarly to what was observed in the iNLE5 underexpressing line (Autran et al. 2002; De Veylder et al. 2001; Hemerly et al. 1995; Mizukami and Fischer 2000; Ullah et al. 2001; Wang et al. 2000). The lack of compensatory cell enlargement in the more severely affected *ScNLE* underexpressing lines therefore suggests that *ScNLE* is not merely involved in the regulation of cell cycle progression but is also required for proper cell enlargement. As discussed below, an implication of *ScNLE* in a basic cellular process such as ribosome biogenesis could give an explanation to the phenotypic consequences of underexpressing *ScNLE*.

Another phenotype associated with *ScNLE* underexpression is a significant increase in the stomatal index (Fig. 4). Stomatal formation has been extensively studied in *Arabidopsis* and similar patterning mechanisms likely apply to other dicots (Geisler et al. 2000). Stomata originate from a meristemoid, a cell with limited stem-cell capacity. The firsts meristemoids produced in an organ originate from some specialized protodermal cells called meristemoid mother cells (MMC). An asymmetric division of the MMC gives rise to a smaller, usually triangular shape meristemoid and a larger neighboring cell. The meristemoid can itself reiterate this pattern of asymmetric division, but only for a limited rounds of cell division, and eventually differentiates into a round guard mother cell (GMC). The GMC finally divides symmetrically to form the pair of guard cells of a stomata. Most of the neighboring cells of a stomatal complex differentiate into pavement cells, but some can reinitiate a stomatal lineage by dividing asymmetrically to give rise to satellite meristemoids. In *Arabidopsis*, almost half of the pavement cells of a leaf are generated through the asymmetric divisions of meristemoids (Geisler et al. 2000). Considering our data on reduced cell proliferation in *ScNLE* underexpressing plants, an increase in stomatal index could be attributed to reduced meristematic maintenance capacity of meristemoid cells. Meristemoids would go through a fewer number of cell divisions before differentiating into GMC and hence less pavement cells would be generated per meristemoid, thus resulting in an increase of the stomatal index.

The *NLE* gene was first isolated as a regulator of the Notch receptor activity in *Drosophila* (Royet et al. 1998) and later, the yeast *NLE* homolog (YCR072c or Rsa4c) was repeatedly found as a non-ribosomal protein associated to pre-60S ribosomal particles (Bassler et al. 2001; Gavin et al. 2002; Nissan et al. 2002). Although no Notch signaling pathway exists in plants and yeasts (Wigge and Weigel 2001), the *NLE* gene is evolutionary conserved in eukaryotes and orthologues are expected to perform similar cellular functions. Ribosome biogenesis seems to be a highly conserved cellular process throughout animals, plants and yeasts (Tschochner and Hurt 2003). In this study, the identification of a homolog of the yeast *MDN1* gene product as a potential protein partner of ScNLE provides further support to the implication of the *NLE* gene in 60S ribosomal subunit biogenesis. With a molecular weight of 560 kDa, MDN1 represents the largest protein identified in the yeast genome. MDN1 consists of an N-terminal ATPase domain, comprised of six AAA^{+}-type promoters, that is separated by a long middle domain from the C-terminal M-domain (Garbarino and Gibbons 2002). The ScNLE–ScMDN1 interaction would involve the Nle domain of ScNLE and the M-domain of ScMDN1, since all the *ScMDN1* clones isolated from the two-hybrid screens contained at least the M-domain but not necessarily the adjacent upstream D/E-rich domain (Fig. 5c). Consistent with this, M-domains are involved in protein-protein interactions and function in multiprotein complexes (Whittaker and Hynes 2002).

Although the ScNLE–ScMDN1 interaction was not confirmed with other protein–protein interaction assays, we believe it is meaningful for the following reasons. First, ScMDN1 was consistently isolated from two different two-hybrid systems, and therefore does not represent an artifact associated to the screening system itself. Second, despite the high number of clones screened, ScMDN1 was the only candidate with a M-domain retrieved. M-domains are present in several other plant proteins and are known to be involved in protein–protein interactions (Liu et al. 2005; Whittaker and Hynes 2002). Third, we have shown that *ScMDN1* shows overlapping expression pattern (Fig. 6) with that determined for *ScNLE* in a previous study (Chantha et al. 2006). Moreover, an ScNLE-GFP protein localized in the nucleus (Fig. 7c), which is in

the same cellular compartment as the yeast MDN1 (Galani et al. 2004; Garbarino and Gibbons 2002) and would therefore provide the potential for these proteins to interact *in planta*. Last, yeast NLE/Rsa4p and MDN1 were repeatedly isolated in the same protein complexes by tandem affinity purification—mass spectrometry using different tagged *trans*-acting factors of pre-60S ribosomal particles (Bassler et al. 2001; Galani et al. 2004; Nissan et al. 2002). The NSA2 protein (YER126p) was also found as a non-ribosomal constituent of these affinity purified pre-60S ribosomal particles (Gavin et al. 2002; Nissan et al. 2002). Interestingly, a homolog of yeast NSA2 was isolated several times with the WDR domain of ScNLE in our two-hybrid screens, bringing further support to the possible involvement of ScNLE in 60S ribosomal subunit biogenesis in plants.

In yeast, 60S ribosomal subunits undergo initial assembly in the nucleolus and then go through different steps of maturation in the nucleoplasm before they are exported to the cytoplasm for final maturation (Tschochner and Hurt 2003). While MDN1 is enriched in a late nucleoplasmic pre-60S ribosomal particle, close to export to the cytoplasm but from which it is released before export (Bassler et al. 2001; Galani et al. 2004), yeast NLE/Rsa4p has been identified in nucleolar, nucleoplasmic and cytoplamic pre-60S particles (Bassler et al. 2001; Nissan et al. 2002). Consistent with this, ScNLE-GFP was here shown to be localized in both the nucleus and cytoplasm of plant cells (Fig. 7), which is also consistent with the subcellular localization determined for the human NLE (Scherl et al. 2002), and yeast NLE/Rsa4p (de la Cruz et al. 2005) orthologs. In yeast, pre-60S particles that are successively formed on their maturation path are composed of substantially different pre-rRNAs species, ribosomal proteins and *trans*-acting factors (Tschochner and Hurt 2003). Based on the structural nature of NLE as a WDR protein, it has been proposed that yeast NLE/Rsa4p could act as a molecular platform for the interaction of other *trans*-acting factors involved in the maturation of pre-60S particles, from early steps in the nucleolus to final dissociation in the cytoplasm (de la Cruz et al. 2005). Taking into account our yeast two-hybrid results and the evolutionary conservation of ribosome biogenesis, NSA2 and MDN1 could represent such *trans*-acting factors that transiently assemble to pre-60S particles through NLE/Rsa4p to accomplish their function.

Depletion of NLE/Rsa4p and MDN1 is yeast causes defects in pre-rRNA processing and pre-60S subunits transport, leading to the reduction of mature 60S subunit formed (de la Cruz et al. 2005; Galani et al. 2004). Because ribosomes are fondamental for global cellular functions, misregulations in ribosomal biogenesis can be expected to cause general developmental defects. In yeast, both *MDN1* and *NLE/Rsa4* are required for cell viability (Giaever et al. 2002). This also seems to be the case for *ScNLE* since fully suppressed plants could not be isolated from transgenic *S. chacoense* lines expressing either an antisense or a RNAi *ScNLE* construct (Chantha et al. 2006). Depletion of NLE/Rsa4p protein in yeast leads to a strong slow-growth phenotype (de la Cruz et al. 2005), which can be compared to the cellular enlargement and proliferation defects observed here on leaf adaxial pavement cells and hence could cause the pleitropic developmental defects in *ScNLE* underexpressing lines. In a previous study, *ScNLE* expression was shown to be upregulated in ovaries by fertilization, an event that induces an intense period of cellular division that initiates fruit development, and its underexpression was shown to cause ovule and seed abortion (Chantha et al. 2006). Reports on the role of genes encoding *trans*-acting factors involved in ribosome maturation during plant development are scarce. An insertion mutation in the *SLOW WALKER1* (*SWA1*) gene, encoding a ribosome *trans*-acting factor, causes a delay in female gametogenesis (Shi et al. 2005). Mutating or silencing of plant ribosomal protein genes produced developmental phenotypes similar to the ones observed in *ScNLE* underexpressing plants, such as reduced organ size and organ number, late flowering and reduced cell proliferation (Lahmy et al. 2004; Popescu and Tumer 2004; Weijers et al. 2001).

In conclusion, our data indicate that *ScNLE* is essential for normal cell proliferation and cell enlargement during plant development. The pleitropic defects in shoot development resulting from underexpressing *ScNLE* is likely the consequence of defects in 60S ribosomal biogenesis.

Acknowledgments We are very grateful to Alexandre Joyeux for providing the GFP vector and for assistance with the confocal microscope. This work was supported by the Natural Sciences and Engineering Research Council of Canada (NSERC) and from the Canada Research Chair program. S.C. Chantha is the recipient of Ph.D. fellowships from NSERC and from Le Fonds Québécois de la Recherche sur la Nature et les Technologies (FQRNT, QC, Canada). D.P. Matton holds a Canada Research Chair in Functional Genomics and Plant Signal Transduction.

References

Agatep R, Kirkpatrick RD, Parchaliuk DL, Woods RA, Gietz RD (1998) Transformation of Saccharomyces cerevisiae by the lithium acetate/single-stranded carrier DNA/polyethylene glycol (LiAc/ss-DNA/PEG) protocol. Technical Tips. Online: http://www.tto.trends.com

Autran D, Jonak C, Belcram K, Beemster GT, Kronenberger J, Grandjean O, Inze D, Traas J (2002) Cell numbers and leaf development in *Arabidopsis*: a functional analysis of the STRUWWELPETER gene. EMBO J 21:6036–6049

Bassler J, Grandi P, Gadal O, Lessmann T, Petfalski E, Tollervey D, Lechner J, Hurt E (2001) Identification of a 60S preribosomal particle that is closely linked to nuclear export. Mol Cell 8:517–529

Bussiere F, Ledu S, Girard M, Heroux M, Perreault J-P, Matton DP (2003) Development of an efficient *cis–trans–cis* ribozyme cassette to inactivate plant genes. Plant Biotechnol J 1:423–435

Chantha SC, Emerald BS, Matton DP (2006) Characterization of the plant Notchless homolog, a WD repeat protein involved in seed development. Plant Mol Biol (in press). DOI 10.1007/s11103-006-9064-4

Clarke AE (1940) Fertilization and early embryo development in the potato. Am Potato J 17:20–25

de la Cruz J, Sanz-Martinez E, Remacha M (2005) The essential WD-repeat protein Rsa4p is required for rRNA processing and intra-nuclear transport of 60S ribosomal subunits. Nucleic Acids Res 33:5728–5739

De Veylder L, Beeckman T, Beemster GT, Krols L, Terras F, Landrieu I, van der Schueren E, Maes S, Naudts M, Inze D (2001) Functional analysis of cyclin-dependent kinase inhibitors of *Arabidopsis*. Plant Cell 13:1653–1668

Esau K (1977) Anatomy of seed plants, 2nd edn. Wiley, New York

Galani K, Nissan TA, Petfalski E, Tollervey D, Hurt E (2004) Rea1, a dynein-related nuclear AAA-ATPase, is involved in late rRNA processing and nuclear export of 60S subunits. J Biol Chem 279:55411–55418

Garbarino JE, Gibbons IR (2002) Expression and genomic analysis of midasin, a novel and highly conserved AAA protein distantly related to dynein. BMC Genom 3:18

Gavin AC, Bosche M, Krause R, Grandi P, Marzioch M, Bauer A, Schultz J, Rick JM, Michon AM, Cruciat CM, Remor M, Hofert C, Schelder M, Brajenovic M, Ruffner H, Merino A, Klein K, Hudak M, Dickson D, Rudi T, Gnau V, Bauch A, Bastuck S, Huhse B, Leutwein C, Heurtier MA, Copley RR, Edelmann A, Querfurth E, Rybin V, Drewes G, Raida M, Bouwmeester T, Bork P, Seraphin B, Kuster B, Neubauer G, Superti-Furga G (2002) Functional organization of the yeast proteome by systematic analysis of protein complexes. Nature 415:141–147

Geisler M, Nadeau J, Sack FD (2000) Oriented asymmetric divisions that generate the stomatal spacing pattern in *Arabidopsis* are disrupted by the too many mouths mutation. Plant Cell 12:2075–2086

Giaever G, Chu AM, Ni L, Connelly C, Riles L, Veronneau S, Dow S, Lucau-Danila A, Anderson K, Andre B, Arkin AP, Astromoff A, El-Bakkoury M, Bangham R, Benito R, Brachat S, Campanaro S, Curtiss M, Davis K, Deutschbauer A, Entian KD, Flaherty P, Foury F, Garfinkel DJ, Gerstein M, Gotte D, Guldener U, Hegemann JH, Hempel S, Herman Z, Jaramillo DF, Kelly DE, Kelly SL, Kotter P, LaBonte D, Lamb DC, Lan N, Liang H, Liao H, Liu L, Luo C, Lussier M, Mao R, Menard P, Ooi SL, Revuelta JL, Roberts CJ, Rose M, Ross-Macdonald P, Scherens B, Schimmack G, Shafer B, Shoemaker DD, Sookhai-Mahadeo S, Storms RK, Strathern JN, Valle G, Voet M, Volckaert G, Wang CY, Ward TR, Wilhelmy J, Winzeler EA, Yang Y, Yen G, Youngman E, Yu K, Bussey H, Boeke JD, Snyder M, Philippsen P, Davis RW, Johnston M (2002) Functional profiling of the *Saccharomyces cerevisiae* genome. Nature 418:387–391

Gietz RD, Woods RA (2002) Transformation of yeast by lithium acetate/single-stranded carrier DNA/polyethylene glycol method. Methods Enzymol 350:87–96

Hemerly A, Engler Jde A, Bergounioux C, Van Montagu M, Engler G, Inze D, Ferreira P (1995) Dominant negative mutants of the Cdc2 kinase uncouple cell division from iterative plant development. EMBO J 14:3925–3936

James P, Halladay J, Craig EA (1996) Genomic libraries and a host strain designed for highly efficient two-hybrid selection in yeast. Genetics 144:1425–1436

Kimble J, Simpson P (1997) The LIN-12/Notch signaling pathway and its regulation. Annu Rev Cell Dev Biol 13:333–361

Koop HU, Steinmuller K, Wagner H, Rossler C, Eibl C, Sacher L (1996) Integration of foreign sequences into the tobacco plastome via polyethylene glycol-mediated protoplast transformation. Planta 199:193–201

Lagacé M, Chantha SC, Major G, Matton DP (2003) Fertilization induces strong accumulation of a histone deacetylase (HD2) and of other chromatin-remodeling proteins in restricted areas of the ovules. Plant Mol Biol 53:759–769

Lahmy S, Guilleminot J, Cheng CM, Bechtold N, Albert S, Pelletier G, Delseny M, Devic M (2004) DOMINO1, a member of a small plant-specific gene family, encodes a protein essential for nuclear and nucleolar functions. Plant J 39:809–820

Lantin S, O'Brien M, Matton DP (1999) Pollination, wounding and jasmonate treatments induce the expression of a developmentally regulated pistil dioxygenase at a distance, in the ovary, in the wild potato *Solanum chacoense* Bitt. Plant Mol Biol 41:371–386

Liu J, Jambunathan N, McNellis TW (2005) Transgenic expression of the von Willebrand A domain of the BONZAI 1/COPINE 1 protein triggers a lesion-mimic phenotype in *Arabidopsis*. Planta 221:85–94

Matton DP, Maes O, Laublin G, Xike Q, Bertrand C, Morse D, Cappadocia M (1997) Hypervariable domains of self-incompatibility RNases mediate allele-specific pollen recognition. Plant Cell 9:1757–1766

Mizukami Y (2001) A matter of size: developmental control of organ size in plants. Curr Opin Plant Biol 4:533–539

Mizukami Y, Fischer RL (2000) Plant organ size control: AINTEGUMENTA regulates growth and cell numbers during organogenesis. Proc Natl Acad Sci USA 97:942–947

Neer EJ, Schmidt CJ, Nambudripad R, Smith TF (1994) The ancient regulatory-protein family of WD-repeat proteins. Nature 371:297–300

Nissan TA, Bassler J, Petfalski E, Tollervey D, Hurt E (2002) 60S pre-ribosome formation viewed from assembly in the nucleolus until export to the cytoplasm. EMBO J 21:5539–5547

Nissan TA, Galani K, Maco B, Tollervey D, Aebi U, Hurt E (2004) A pre-ribosome with a tadpole-like structure functions in ATP-dependent maturation of 60S subunits. Mol Cell 15:295–301

O'Brien M, Kapfer C, Major G, Laurin M, Bertrand C, Kondo K, Kowyama Y, Matton DP (2002) Molecular analysis of the stylar-expressed *Solanum chacoense* small asparagine-rich protein family related to the HT modifier of gametophytic self-incompatibility in Nicotiana. Plant J 32:985–996

Parchaliuk DL, Kirkpatrick RD, Agatep R, Simon SL, Gietz RD (1999) Yeast two-hybrid system screening. Technical Tips. Online: http://www.tto.trends.com

Popescu SC, Tumer NE (2004) Silencing of ribosomal protein L3 genes in *N. tabacum* reveals coordinate expression and significant alterations in plant growth, development and ribosome biogenesis. Plant J 39:29–44

Royet J, Bouwmeester T, Cohen SM (1998) Notchless encodes a novel WD40-repeat-containing protein that modulates Notch signaling activity. EMBO J 17:7351–7360

Scherl A, Coute Y, Deon C, Calle A, Kindbeiter K, Sanchez JC, Greco A, Hochstrasser D, Diaz JJ (2002) Functional proteomic analysis of human nucleolus. Mol Biol Cell 13:4100–4109

Shi DQ, Liu J, Xiang YH, Ye D, Sundaresan V, Yang WC (2005) SLOW WALKER1, essential for gametogenesis in *Arabidopsis*, encodes a WD40 protein involved in 18S ribosomal RNA biogenesis. Plant Cell 17:2340–2354

Smith TF, Gaitatzes C, Saxena K, Neer EJ (1999) The WD repeat: a common architecture for diverse functions. Trends Biochem Sci 24:181–185

Tschochner H, Hurt E (2003) Pre-ribosomes on the road from the nucleolus to the cytoplasm. Trends Cell Biol 13:255–263

Tsukaya H (2002) Interpretation of mutants in leaf morphology: genetic evidence for a compensatory system in leaf morphogenesis that provides a new link between cell and organismal theories. Int Rev Cytol 217:1–39

Ullah H, Chen JG, Young JC, Im KH, Sussman MR, Jones AM (2001) Modulation of cell proliferation by heterotrimeric G protein in *Arabidopsis*. Science 292:2066–2069

van Nocker S, Ludwig P (2003) The WD-repeat protein superfamily in *Arabidopsis*: conservation and divergence in structure and function. BMC Genom 4:50

Wang H, Zhou Y, Gilmer S, Whitwill S, Fowke LC (2000) Expression of the plant cyclin-dependent kinase inhibitor ICK1 affects cell division, plant growth and morphology. Plant J 24:613–623

Weijers D, Franke-van Dijk M, Vencken RJ, Quint A, Hooykaas P, Offringa R (2001) An *Arabidopsis* minute-like phenotype caused by a semi-dominant mutation in a RIBOSOMAL PROTEIN S5 gene. Development 128:4289–4299

Whittaker CA, Hynes RO (2002) Distribution and evolution of von Willebrand/integrin A domains: widely dispersed domains with roles in cell adhesion and elsewhere. Mol Biol Cell 13:3369–3387

Wigge PA, Weigel D (2001) *Arabidopsis* genome: life without notch. Curr Biol 11:R112–R114

Williams EJ (1955) Seed failure in the Chippewa variety of *Solanum tuberosum*. Bot Gaz 10:10–15